ABSTRACT

Title of Thesis: **INVESTIGATING THE INTERACTIONS BETWEEN BIOPOLYMERS AND BLOOD VIA OPTICAL MICROSCOPY.**

Ian Collins MacIntire, Master of Science, 2015

Directed by: Prof. Srinivasa R. Raghavan
Department of Chemical & Biomolecular Engineering

Hydrophobically modified (hm) derivatives of biopolymers such as chitosan have been shown to convert liquid blood into an elastic gel. This interesting material property could make hm-chitosan (hmC) useful as a hemostatic agent in treating severe bleeding. In this work, we attempted to probe the mechanism of action of hmC by studies on mixtures of blood cells and hmC using optical microscopy. Our results show that the presence of hydrophobic tails on hmC induces significant clustering of blood cells. We show that clustering increases as the fraction of hydrophobic tails on hmC increases, length of the hydrophobic tails increases, and as concentration of hmC increases. Finally, clustering due to hmC could be reversed by the addition of the supramolecule α-cyclodextrin, which is known to capture hydrophobes in its binding pocket. The results from this work support the earlier mechanism, with a few important modifications.

INVESTIGATING THE INTERACTIONS BETWEEN BIOPOLYMERS AND BLOOD VIA OPTICAL MICROSCOPY

By

Ian Collins MacIntire

Thesis submitted to the Faculty of the Graduate School of the
University of Maryland, College Park, in partial fulfillment
of the requirements for the degree of
Master of Science
2015

Advisory Committee:

Prof. Srinivasa R. Raghavan, Dept. of Chemical & Biomolecular Engineering, Chair

Prof. Ganesh Sriram, Dept. of Chemical & Biomolecular Engineering

Prof. Pangiotis Dimitrakopoulos, Dept. of Chemical & Biomolecular Engineering

Dedication

I dedicate this thesis to my wife. Thanks for motivating me to do it.

Acknowledgements

I would first like to acknowledge Dr. Raghavan for making this opportunity possible and for all the guidance he has provided throughout the process of completing this degree. If it were not for him, I would have not attempted to do anything like this.

I would second like to acknowledge Dr. Matthew Dowling for all of his support and guidance during this process as well. I really appreciate the support and flexibility he has shown for me in order to complete this process.

Third I would like to acknowledge Dr. John Gustin for tremendous support during the difficult writing phase of this thesis. I probably would not have been able to complete the writing of my thesis without John's advice in that area.

I also would like to acknowledge all the current and former members of the complex fluids group such as Brady, Ankit, Ankit, Veena, Annie, Jasmin, Charles, Salimeh, Vishal, Hyuntaek, Kunal, Chanda, Kevin, Joe, and Bani. Thank you all for the valuable information and guidance you have provided to me throughout this process.

I would like to acknowledge Dr. Ian White for allowing me to use his microscope and cell culture facility, and to Dr. White's graduate students for helping me troubleshoot problems in the cell lab.

Finally, I would to acknowledge all of the undergraduate students who have helped me over the years: Karl, Erica, Bo, Tia, Evelyn, Stokes, Shekhar, Olivia, and Seung. Your help was extremely valuable in allowing me to get everything done on a daily basis.

Table of Contents

List of Figures

Chapter 1: INTRODUCTION & OVERVIEW

The motivation for the current work comes from recent studies that have been published on a class of polymers called "associating" polymers. These are polymers that have a hydrophilic backbone and hydrophobic side-chains ("tails") that are tethered to the backbone.[1,2] The hydrophobic tails on adjacent polymer chains will tend to associate with each other via hydrophobic interactions, and as a result, these polymers have the ability to thicken aqueous solutions.[1,3] Moreover, these polymers also tend to have strong interactions with different types of colloidal and self-assembled structures.[1,2,4-13]

In our laboratory, we have focused on associating polymers derived by attaching hydrophobic tails to common biopolymers such as chitosan and alginate. Much of our work has been done with chitosan, which is a cationic polysaccharide that is itself derived from chitin. Chitin is the second most abundant biopolymer in nature following cellulose, and it is found in the hard shells of insects and crustaceans like crabs and shrimp.[14] While chitin is insoluble in water, it can be deacetylated to give chitosan, which is soluble under acidic conditions due to the presence of charged amine groups. We convert chitosan into an associating polymer by attaching *n*-alkyl tails to some of the amines along the polymer backbone.[9,10,12,13,15] The resulting polymer is termed hydrophobically modified chitosan (hmC).

We have studied hmC in conjunction with structures covered by lipid membranes, including vesicles and biological cells.[9,10,12,13,15] First, we showed that when hmC was

added to a solution of vesicles (~ 100 nm in diameter), the thin liquid was converted into an elastic gel.[13] Thereafter, we demonstrated similar gelation when hmC was mixed with liquid blood (either human or bovine).[10] Gelation was confirmed by rheological techniques (Figure 1.1). Note that blood cells are several microns in diameter, i.e., they are much larger than the vesicles. Also, it is important to mention that we added heparin or sodium citrate to the blood to prevent its coagulation via the blood clotting cascade. Thus, gelation of blood by hmC was not related to biochemical pathways. We also showed that gelation by hmC required the presence of the blood cells; in contrast, gelation did not occur when hmC was added to the protein component of blood, i.e., blood plasma. Moreover, hmC also gelled other kinds of biological cells including mammalian endothelial cells.[15]
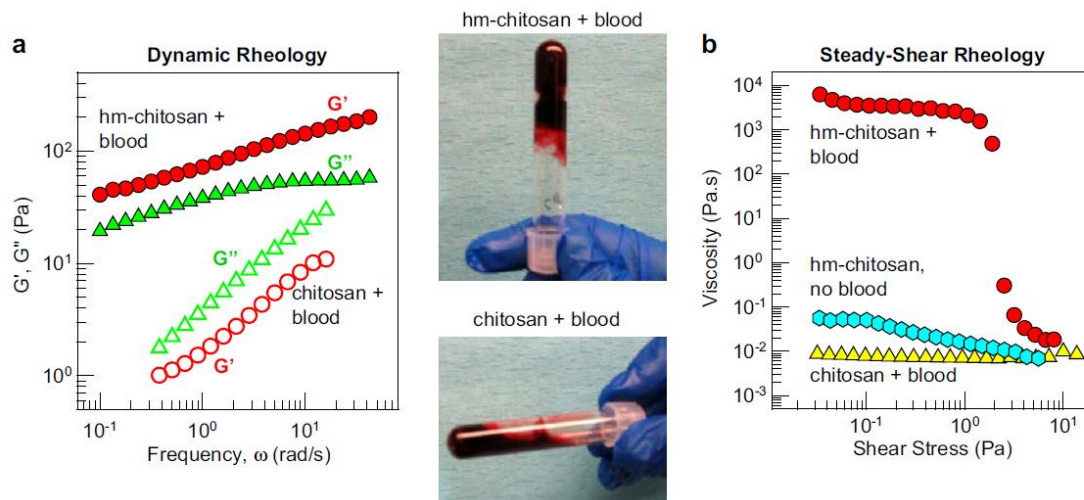
Figure 1.1 Visual observations and rheological data showing that hmC gels blood whereas chitosan does not. Here, hmC and chitosan (0.25 wt%) are added to heparinized human blood. The hmC /blood mixture holds its weight in the inverted tube whereas the chitosan/blood mixture is a freely flowing liquid. In (a) dynamic rheological data for the elastic modulus G' and the viscous modulus G'' vs. frequency ω are shown for the two samples. The hmC sample (closed symbols) displays the rheology of a gel ($G' > G''$)

2

whereas the chitosan sample (open symbols) responds like a viscous sol. In (b) steady-shear rheological data for the viscosity vs. shear stress are shown. The hmC/blood mixture (red circles) shows a significantly higher viscosity relative to both the chitosan/blood mixture (yellow triangles) as well as a 0.25 wt% solution of hmC alone.

The mechanism for the gelation of microscale cells of blood (as well as nanoscale vesicles) by hmC has been hypothesized to involve *hydrophobic interactions*.[10,13] Specifically, some of the hydrophobic tails on hmC are expected to get inserted into the membranes of blood cells. Thereby, the same hmC chain could become bound to more than one cell, i.e., the chain could bridge adjacent cells. Such bridging would result in a sample-spanning three-dimensional (3-D) network of cells connected by polymer chains (see Figure 2.2 in Chapter 2), which can explain the gel-like behavior of the sample.

Support for the above mechanism comes from various related experiments. For example, other associating polymers, including hydrophobically modified alginate (hmA), hydrophobically modified polyethylene oxide (hm-PEO), and hydrophobically modified hydroxyethylcellulose (hm-HEC) have also been shown to form gels when mixed with blood, other cells, or vesicles.[15-19] Moreover, our laboratory has shown that gelation of blood (or vesicles) by hmC can be reversed by adding alpha-cyclodextrin (α-CD), a barrel-shaped supramolecule with a hydrophobic binding pocket.[10,15] Such reversal is hypothesized to occur because α-CD molecules can sequester the hydrophobes on hmC within their binding pockets, thereby preventing the chains from connecting adjacent cells. Thus, the very fact that α-CD works as an ungelling agent points to hydrophobic interactions as being responsible for gelation in the first place.

The gelling of blood by hmC is not just of academic interest. This property suggests that hmC could serve as a hemostatic agent and prevent bleeding from traumatic injuries. Traumatic injury is a significant source of mortality worldwide with an estimated rate of 70 per 100,000 of the population in 2013.[20] In the US, trauma is now the leading cause of death for those 46 and under.[21] A major cause of these trauma deaths is uncontrolled hemorrhage in both the civilian and military arena.[22-26] To test the hemostatic ability of hmC, we collaborated with surgeons at the University of Maryland Medical School. We showed that hmC-based solid dressings can arrest even the most severe of bleeds (such as injuries to the femoral artery in pigs) whereas native chitosan was unable to contain the same bleeds.[27] In addition, hmC-based foams have also been shown to act as hemostatic agents against liver injuries in pigs.[28,29] Thus, hmC has significant potential as a hemostatic agent.

Although the exact mechanism for hemostatic action by hmC-based dressings and foams is still not understood, we believe it is at least partly connected to the blood-gelling ability of hmC. This brings us to the mechanism for blood gelling. While the postulated mechanism (in terms of hydrophobic interactions) is reasonable, the evidence for it has been mostly indirect. There is still a need to substantiate this mechanism by directly probing the microstructure in hmC-blood mixtures. Since blood cells are microscale structures, they can be directly visualized by optical microscopy. We therefore set out to study the interactions between blood cells and hmC using bright-field optical microscopy. Results for hmC are compared with those for the parent chitosan. Important variables in our study include the degree of hydrophobic modification, the polymer molecular-weight,

and the polymer concentration. In addition, we also study hmC-blood mixtures after the addition of various cyclodextrins. Overall, the results from this work support the earlier mechanism, but they do suggest a few important modifications.

Chapter 2: BACKGROUND

2.1 Chitosan

Chitosan is a linear polysaccharide that is derived from chitin (poly-N-acetyl-glucosamine) (structure in Figure 2.1a). To produce chitosan, chitin is first extracted from the shells of crustaceans such as crabs and shrimp. Then chitin is deacetylated under basic conditions to give chitosan. Deacetylation is usually incomplete, leaving a small percentage of the N-acetyl groups along the polymer backbone. The number of remaining N-acetyl groups remaining on chitosan is expressed as degree of acetylation (DA). DA is the percentage of glucosamine units that are still bound to an N-acetyl group. DA values of commercially available chitosans typically range from 30% down to 1%.[30-32] The structure of chitosan is shown below, along with a schematic representation. (Figure 2.1). To dissolve chitosan in an aqueous solution, the amines along its backbone need to be protonated. Thus, a pH below 6.5 is required for chitosan to be soluble. Many acids can be used to achieve this pH, with acetic acid being the most common choice. When the amine groups are protonated, chitosan becomes a cationic polymer. [30-32]
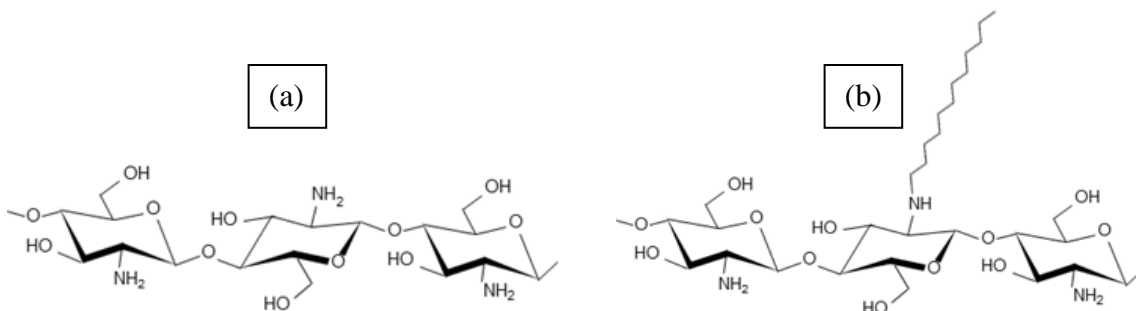
Figure 2.1 Chemical structure of (a) chitosan and (b) hydrophobically modified chitosan (hmC) with *n*-dodecyl (C$_{12}$) hydrophobic side chains.

Chitosan has many interesting and useful properties. It is currently used commercially in a variety of applications, including water treatment, food preservation, dietary pills and supplements, antibacterial coatings, and bioseparation membranes. [14,30] Also, it is considered biocompatible and has been used in medical applications such as drug delivery, tissue engineering, and wound care. [30,33] Chitosan also has antimicrobial properties and has been shown to be effective against a range of bacteria. [31,34] Chitosan is also used extensively in hemostatic products. It is thought that chitosan acts as a mucoadhesive, which creates a mechanical barrier at the injury site, thus reducing blood loss from the wound and helping the body form a natural clot to fully stop the bleeding.[35] However, the hemostatic efficacy of native chitosan has been called into question in several studies, including ours.[27-29]

2.2 Hydrophobically Modified Chitosan

Hydrophobically modified chitosan (hmC) is produced by reacting aldehydes with the amine groups on chitosan via reductive amination.[10,13] In the process, the amine (NH_2) groups are converted into NH-R groups, where R is the moiety attached to the aldehyde. Typically, R is an *n*-alkyl moiety ranging from C_6 to C_{12}. The structure of hmC with C_{12} hydrophobic tails is shown in Figure 2.1b. A typical procedure for synthesizing hmC with C_{12} tails involves the following steps. First, *n*-dodecyl aldehyde is added to an acidic chitosan solution in a water-ethanol mixture, followed by addition of sodium cyanoborohydride. The molar ratio of aldehyde to chitosan monomer(s) is fixed at a certain value (e.g. 2.5%). The reaction yields the hmC, which is then precipitated by raising the pH and adding ethanol. Next, the precipitate is purified by washing with

ethanol followed by deionized water. The final hmC precipitate is re-dissolved in acetic acid solution and the concentration is recalibrated. This solution tends to be viscous due to associations between the hydrophobes (this is a qualitative indication that the synthesis has been successful). The degree of hydrophobic modification (i.e., the amines with a hydrophobic unit divided by the total available amines) tracks the value expected from stoichiometry, and this can be confirmed using ^{1}H NMR. Typical levels of modification are between 1-5%. At these low levels, hmC is still soluble in aqueous solution.
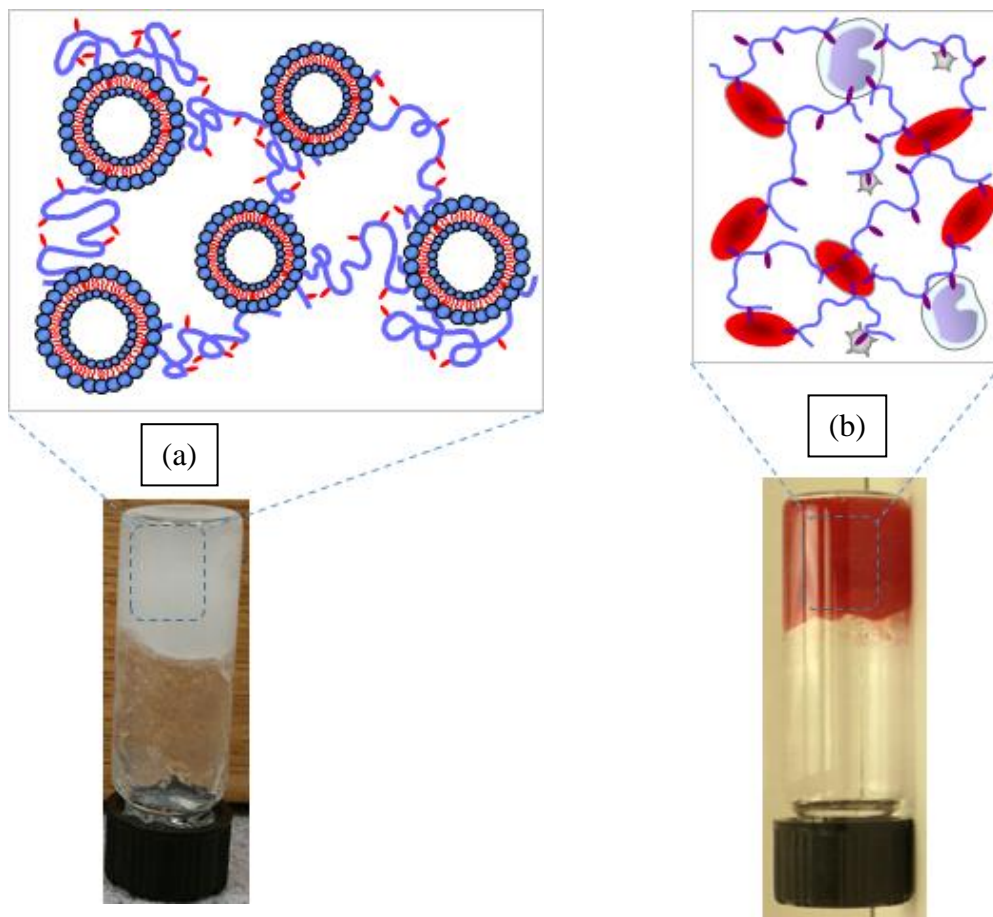
Figure 2.2 Photographs of gels obtained by combining hmC with (a) vesicles; and (b) citrated bovine blood. In both cases, the gels hold their weight in the inverted vials. Schematics of the microstructure in each gel is also shown. It is hypothesized that the hmC chains insert their hydrophobes into the membranes of vesicles or blood cells, leading to a sample-spanning network of structures connected by polymer chains.

2.3 Studies on hmC Combined with Vesicles, Blood, Mammalian Cells

Our lab has previously shown that a gel is formed when a solution of hmC is mixed with a solution of cationic surfactant vesicles.[13] Examination of the resulting gels using small-angle neutron scattering and cryo-TEM confirms that the vesicles remain intact during the formation of the gel. Based on both these findings and the observation that unmodified chitosan does not form a similar gel with the vesicles, it was hypothesized that the mechanism for gelation between hmC and cationic vesicles involves insertion of the hydrophobic groups on the hmC backbone into the vesicle bilayers. This creates a 3-dimensionally crosslinked network that immobilizes the hmC polymer chains and results in an elastic gel. A picture of a typical hmC/vesicle gel and a schematic representation of the gel network is shown above in figure 2.2(a).[13]

In addition our lab has previously reported that when hmC is mixed with blood, the mixture also forms a gel.[10] In contrast, unmodified chitosan does not result in gelation when mixed with blood. We previously proposed a mechanism for the gelation of hmC with blood which paralleled that proposed for vesicles. This mechanism is that the hydrophobic groups from hmC insert themselves into the blood cell membranes forming a network of crosslinks as shown above in figure 2.2(b).[10]

The gelation properties of hmC can be extended to cell types other than blood cells, as shown by Javvaji et. al.[15] In this work, suspensions of human MCF7 breast cancer cells and human umbilical vein endothelial cells (HUVECs) were gelled by mixing with solutions of hmC. The reported rheological profile of the cell/hmC gels showed very similar characteristics to the data with bloods cells shown in figure 1.1.

This ability to gel various types of cells could have important applications in fields such as tissue engineering and cell culture.

Interestingly, the gelation of vesicles, blood cells, and mammalian cells can all be reversed by the addition of a molecule called alpha-cyclodextrin (α-CD).[10,15] Upon addition of α-CD, the mixtures will once again become free-flowing liquids. α-CD is a largely hydrophilic molecule, but it uniquely contains a small hydrophobic inner pocket. We have previously suggested that reversal of gelation is due to the hydrophobes on the hmC being sequestered into the hydrophobic pockets of the α-CD molecules. Such sequestration consequently displaces the hydrophobes from the bilayers and reverses the physical gelation. A schematic of this process is shown below in figure 2.3.
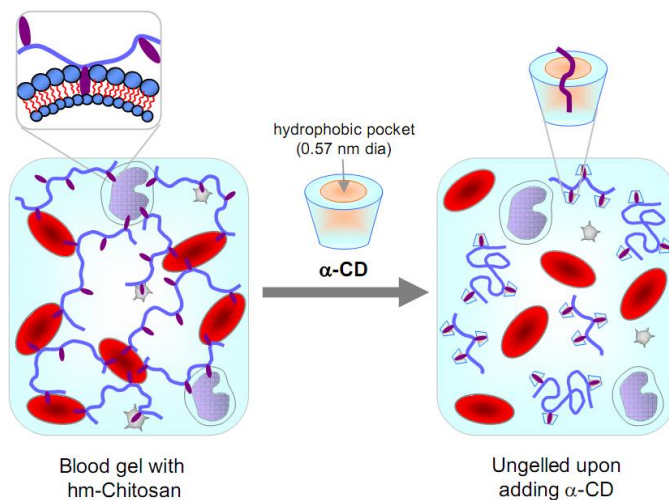
Figure 2.3 Schematic mechanism of ungelling induced by α-CD: the hydrophobes on the polymer are disengaged from cell membranes and instead sequestered within the hydrophobic cavities of the α-CDs.

2.4 Optical Microscopy and Image Analysis

The main technique used in this work is bright-field optical microscopy. Microscopy is a technique used to visualize things that are below the resolution of the human eye using optical lenses for magnification. Microscopes work by focusing light through a series of lenses, resulting magnifications of 100x to over 1000x. There is a limit to the magnifying ability of microscopes, however, as the diffraction of light through the microscope's aperture becomes significant as the size of the object being observed approaches the wavelength of the light being used to see it.[36]

Sample contrast is an important factor in microscopic imaging. Samples that exhibit strong contrast against their surroundings can be easily imaged using standard bright field microscopy in which light is transmitted through the sample, and the sample's contrast relative to the background makes it clearly visible. In the case of highly translucent samples which exhibit poor contrast, a technique known as phase contrast enhancement may be employed. This technique separately manipulates the transmitted and scattered light to artificially enhance contrast.[36,37]

Once microscopic images are collected, the images may need to be systematically analyzed to extract quantitative data related to the sample. The process for obtaining data from images is known as image analysis. The basic goal of image analysis is primarily to count and measure objects (such as particles or biological cells) that are present in a microscopic image. This involves the recognition by the software of each individual object's size and shape.[37]

Image analysis can be performed using a series of steps. The first steps are visualization on a microscope, and image capture by an associated camera. The resulting image is then processed by converting to grey scale (if not already captured in grey scale), segmentation of the various particles in the image, and binary processing in which data is generated based on the particles in the image. The measurements are reported as numerical data, which can then be analyzed and interpreted as appropriate for the particular sample type under investigation. This process is represented schematically by the following figure 2.4 taken from Pons and Vivier.[37]
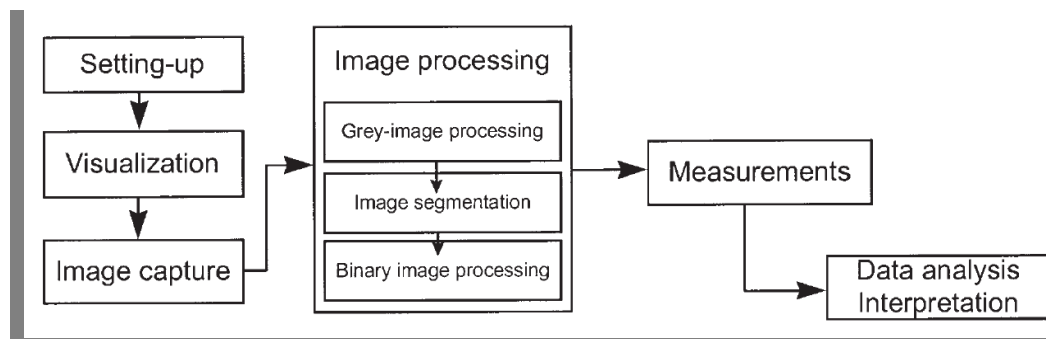
Figure 2.4 The flow of the image analysis process

2.5 Rheology

A second technique used in this thesis is rheology. Rheology is formally defined as the study of flow and deformation in materials. Rheological measurements provide information on the relation between microstructure and macroscopic properties. These measurements are typically performed on a rheometer under steady or dynamic oscillatory shear. Typical geometries used in rheometers are the cone-and-plate, the parallel plate, and the concentric cylinder or Couette.

12

In *steady shear rheology*, the sample is subjected to a constant shear-rate $\dot{\gamma}$ (e.g. by applying a continuous rotation at a fixed rate on a rotational instrument), and the response is measured as a shear-stress σ. The ratio of shear-stress σ to shear-rate $\dot{\gamma}$ is the (apparent) viscosity η. A plot of the viscosity vs. shear-rate $\dot{\gamma}$ is called the flow curve of the material.

In *dynamic or oscillatory rheology*, a sinusoidal strain $\gamma = \gamma_0 \sin(\omega t)$ is imposed on the sample. Here, γ_0 is the strain-amplitude (i.e. the maximum applied deformation) and ω is the frequency of the oscillations. The sample response will be in the form of a sinusoidal stress $\sigma = \sigma_0 \sin(\omega t + \delta)$ which will be shifted by a phase angle δ with respect to the strain waveform. Using trigonometric identities, this stress waveform can be decomposed into two components, one in-phase with the strain and the other out-of-phase by 90°:

$$\sigma = G'\gamma_0 \sin(\omega t) + G''\gamma_0 \cos(\omega t) \tag{2.1}$$

Here, G' is the elastic modulus and it provides information about the elastic nature of the material. Since elastic behavior implies the storage of deformational energy, G' is also called the storage modulus. On the other hand, G'' is the viscous modulus and it characterizes the viscous nature of the material. Since viscous deformation results in the dissipation of energy, G'' is also called the loss modulus. For these properties to be meaningful, the dynamic measurements must be made in the "*linear viscoelastic*" (LVE) regime of the sample. This means that the stress must be linearly proportional to the

imposed strain (i.e., moduli independent of strain amplitude). In that case, the elastic and viscous moduli are only functions of the frequency of oscillations ω, and are true material functions. A log-log plot of the moduli vs. frequency, i.e. $G'(\omega)$ and $G''(\omega)$, is called the frequency spectrum of the material, and it is a signature of the material microstructure.

Chapter 3: INVESTIGATING THE INTERACTIONS BETWEEN BIOPOLYMERS AND BLOOD USING OPTICAL MICROSCOPY

3.1 Introduction

The goal of this thesis is to study the interactions between hydrophobically modified chitosan (hmC) and blood using bright-field optical microscopy. As mentioned previously, hmC has been shown to convert liquid blood into a gel, and the mechanism is believed to involve hydrophobic interactions.[10] That is, hydrophobes on hmC are believed to embed in the membranes of blood cells, thereby connecting adjacent cells into a 3-D network (see schematic in Figure 2.2b). Thus far, no direct evidence for this mechanism has been obtained, i.e., there have been no direct or *in situ* studies into the microstructure of hmC/blood mixtures.

Blood is a combination of different cell types (red cells, white cells, platelets), but the red blood cells (RBCs) are by far the most abundant and these typically have diameters of about 6-8 μm.[38] Thus, blood cells can be directly visualized by optical microscopy. In our experiments, we add hmC to blood and observe the mixtures under the microscope for distinct perceptible changes. Our principal finding is that hmC induces blood cells to aggregate into large clusters. We correlate the extent of clustering as a function of different variables including the degree of hydrophobic modification of the hmC, the hmC molecular-weight, and the hmC concentration. In addition, we also study hmC-blood mixtures after the addition of various cyclodextrins (CDs) to probe

whether the CDs have an effect on the extent of clustering. Overall our work provides further insight into hmC/blood interactions and this leads us to propose a few modifications to the current mechanism for blood gelation.

3.2 Experimental

Materials. Chitosan (99% deacetylated) was purchased from Primex (Iceland). Dodecyl aldehyde and sodium cyanoborohydride were obtained from Sigma Aldrich. Alpha-cyclodextrin (α-CD), methyl-beta-cyclodextrin (mβ-CD), and hydroxypropyl-beta-cyclodextrin (hpβ-CD) were obtained from TCI America. Citrated bovine whole blood was obtained from Lampire Biological Laboratories. Mouse fibroblast L929 cells were obtained from ATCC, as were reagents for cell culture, including Eagle's MEM culture media, fetal bovine serum (FBS), and penicillin-streptomycin solution.

Synthesis. hmC was synthesized using a procedure based on previous methods.[10,13] Briefly, chitosan was dissolved at 1% w/v in a 0.2 M acetic acid solution. An equal volume of ethanol was then added as a co-solvent before the temperature was increased to 55°C. Varying amounts of *n*-alkyl aldehyde were dissolved in ethanol and mixed into the chitosan solution to give varying levels of hydrophobic modification (0.5, 1.0, 2.0, 5.0 mol%, relative to the amines). The reaction mixture was treated with an aqueous solution of sodium cyanoborohydride, and left to react overnight. The hmC was precipitated by raising the pH of the mixture to around 10. The precipitate was purified by multiple washes of ethanol and water, and then dried to a powder.

16

Solution Preparation. hmC was dissolved in 0.04 M acetic acid solution at various concentrations. Sodium chloride was then added at a concentration of 0.9% w/v for osmotic balance. The bovine blood was diluted (10×) with normal saline.

Cell Suspension Preparation. ATCC L-929 mouse fibroblasts were cultured in Eagle's MEM media supplemented with 5% FBS, 50 IU/mL penicillin, and 0.05 mg/mL streptomycin. Cells were harvested, pelleted by centrifugation, and resuspended to give a cell concentration of approximately 2×10^7 cells/mL in normal saline.

Optical Microscopy. To prepare a sample for microscopic observation, 20 µL of the hmC solution was pipetted onto a glass slide. 20 µL of 10× diluted blood was then added. The combined solutions were mechanically mixed with a stirring rod, and a coverslip was placed on top of the sample. Samples were then imaged immediately using an Olympus IX51 at 100× and 400× magnification. A Hamamatsu A3472-06 camera was used to capture multiple micrographs for each sample.

Image Analysis. Clustering in the samples was analyzed using the ImageJ program. Images were thresholded and subjected to the ImageJ particle analyzer function. The sizes of all clusters greater than 48 µm^2 was recorded for each sample. For a given sample, several parameters were calculated to obtain an estimate for the extent of clustering, including the average size of the ten largest clusters, and the fraction of the image area occupied by the ten largest clusters.

3.3 Results and Discussion

We performed experiments with bovine blood that has been treated with sodium citrate, which is a known inhibitor of the clotting cascade. The elimination of any interference from the clotting cascade is important for our experiments. Another inhibitor of blood clotting is the biopolymer, heparin. As demonstrated previously, hmC can gel both citrated as well as heparinized blood. This implies that gelation has no connection to the clotting cascade. Here, we chose to use citrated blood for all our experiments. One reason for this is that heparin is a highly negatively charged macromolecule that can interact via electrostatic interactions with chitosan as well as hmC, which are both cationic polymers. Thus, by using citrated blood we avoid some complications due to electrostatic effects, which makes our results cleaner and easier to interpret.

The protocol for our microscopic studies involves combining 20 µL of hmC solution with 20 µL of citrated blood on a microscope slide, quickly mixing the two on the slide, and observing immediately by bright-field microscopy. In the hmC solution, we included 0.9% wt/vol of NaCl for osmotic balance with blood cells. This is important to ensure that the blood cells do not suffer any osmotic shock upon mixing with the hmC solution. With regard to the blood, we diluted the original stock solution by 10× in normal saline. This was done because we found that at the original concentration, the density of blood cells was too high within the microscopic field of view, which made it difficult to distinguish if the cells were lying on top of each other or undergoing aggregation. With the diluted blood, the cells could be resolved better, as shown below.
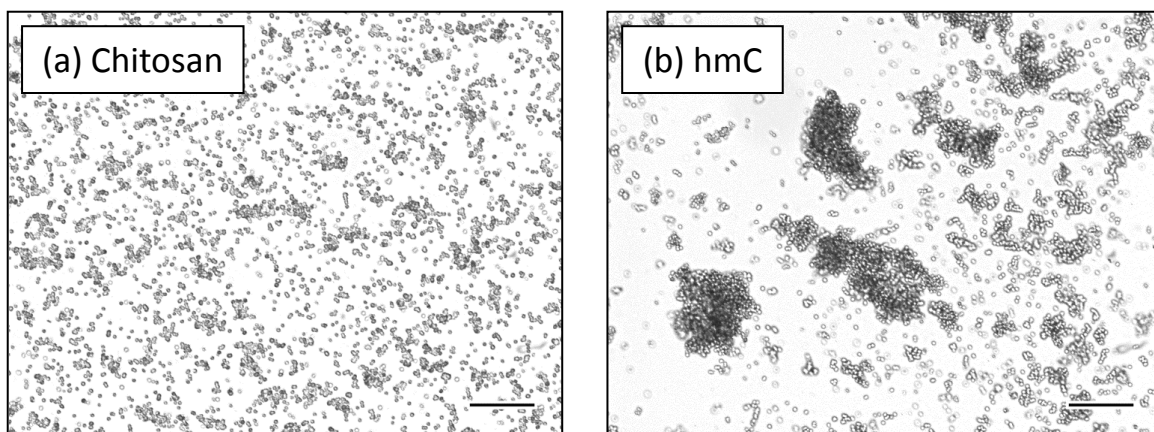
Figure 3.1 Interactions of citrated bovine blood with 0.05 wt% chitosan (a) and hmC (b). The hmC has C_{12} hydrophobes with the degree of modification being 5 mol%. Scale bars are 100 μm.

Figure 3.1 shows representative images at 100× magnification of a mixture of the above blood with 0.05 wt% hmC or chitosan. These two images illustrate the key difference between the two polymers. In the case of chitosan, the blood cells are mostly discrete structures (Figure 3.1a). There seem to be a few small clusters of cells, although it is not clear if these are truly clusters (i.e., cells that are adhered to one another) or if the cells are simply overlapping at the same spot in the image, but unconnected to each other. In comparison, the majority of cells in the hmC case are clustered (Figure 3.1b). The clusters are dense structures and consequently appear dark in the image. Also, note that because much of the cells are in clusters, there is a lot of "empty" space in the image where no cells are seen. Thus, *we infer that hmC induces blood cells to cluster, while chitosan does not*. A closer look at the blood cell clusters induced by hmC is shown in the two images of Figure 3.2. It is evident that the clusters are dense aggregates of the cells. The individual clusters each have an area of more than 3000 $μm^2$ and their shape is

irregular. Also, note that there is no obvious disruption or hemolysis of the cells, i.e., all

the cells in the clusters appear to be intact structures.
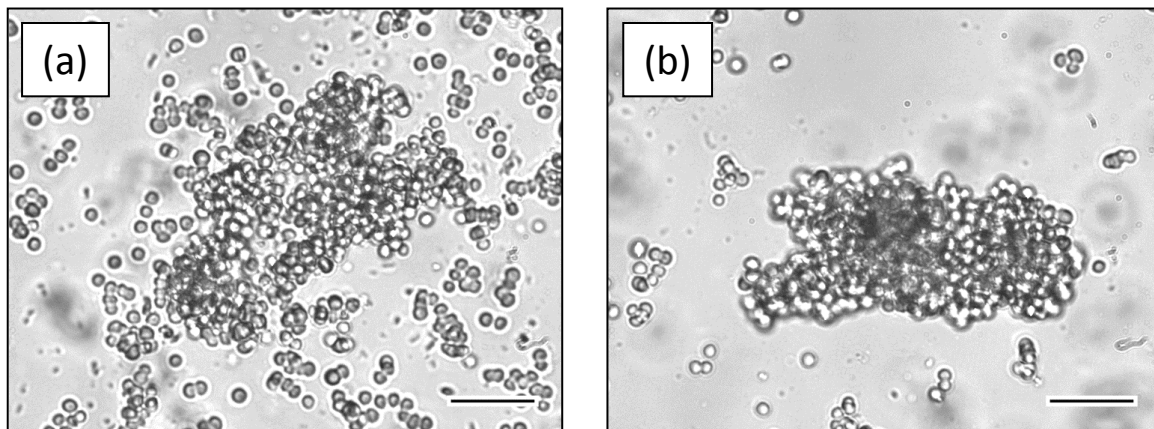
Figure 3.2 Close-ups (400× magnification) of blood cell clusters formed by combining citrated bovine blood with 0.05 wt% hmC (C_{12}, 5 mol%). Scale bars are 30 μm.
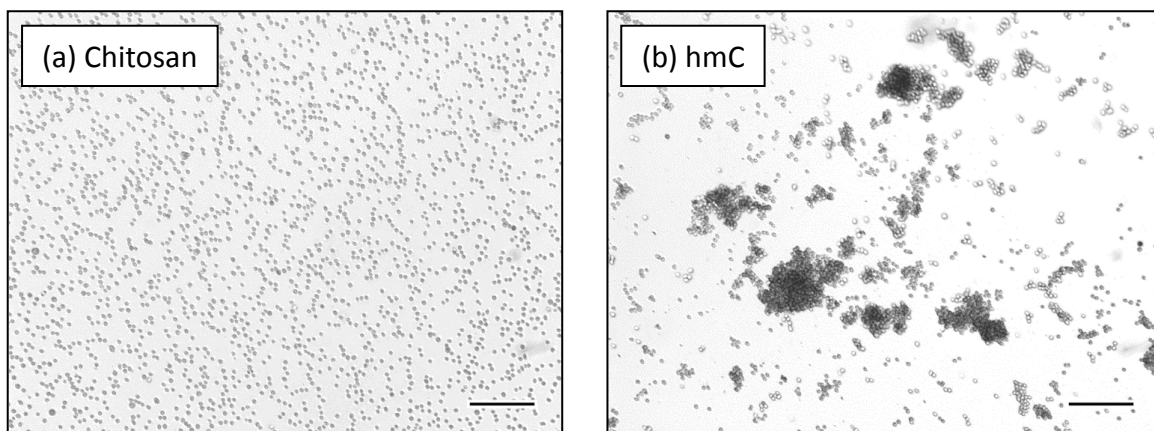
Figure 3.3 Interactions of L-929 mouse fibroblast cells with 0.05 wt% chitosan (a) and hmC (C_{12}, 5 mol%) (b). Scale bars are 400 μm.

Similar results were also obtained with cells other than blood. For example, we

studied L-929 mouse fibroblast cells, which were resuspended at a concentration of about

2×10^7 cells/mL in normal saline. This cell suspension was combined with 0.05 wt% hmC or unmodified chitosan. We again observe that the cells remain as discrete structures when combined with chitosan (Figure 3.3a) whereas they are aggregated into large and dense clusters when combined with hmC (Figure 3.3b).

Figure 3.1a   Figure 3.1b
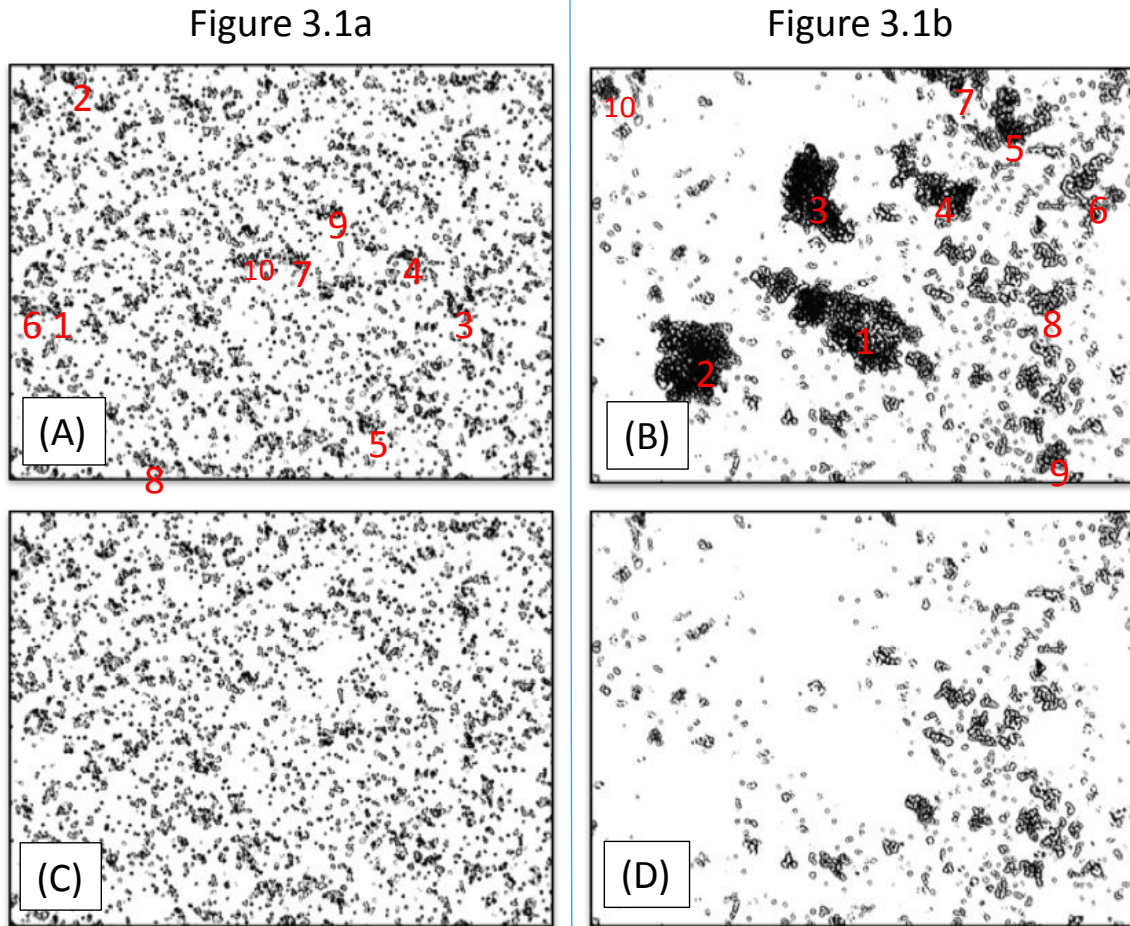
Figure 3.4 Analysis of the images in Figure 3.1 showing the interaction of bovine blood with 0.05 wt% chitosan and hmC. (A) and (B) are thresholded versions of Figure 3.1a and 3.1b, respectively. The 10 largest clusters in these images are identified. (3) and (4) are the same images after removing the 10 largeest clusters. Note that (C) seems nearly identical to (A), whereas (D) is very different from (C). That is, the 10 largest clusters occupy only ~ 5% of the total area in Figure 3.1a whereas they occupy ~ 62% of the area in Figure 3.1b.

Before proceeding further, we discuss measures to quantify the differences between images of clustered and unclustered cells, such as in Figure 3.1. We used the

ImageJ software to perform the requisite calculations. The software can threshold the image and identify the outlines of all "clusters" (defined as those of size > 48 µm^2, which is the approximate area of a single RBC) and thereby also make a cluster size distribution. However, as noted above, it is not clear in the case of the chitosan sample whether the structures identified are indeed clusters or if the cells are merely overlapping. For this reason, measures such as the fraction of cells in clusters or the average sizes of clusters were not reliable.

The procedure we chose to use is depicted in Figure 3.4. First, we threshold the image and identify the 10 largest clusters using ImageJ. The 10 largest clusters in Figure 3.1a and 3.1b (in decreasing order of size) are numbered in (A) and (B) of Figure 3.4. Next, we show the same fields of view in (C) and (D) after the 10 clusters are removed. Note that (D) looks very different from (B) because the 10 clusters occupied a large fraction of the area in (B), whereas (C) and (A) look about the same because the 10 clusters were a small fraction of the area. This tells us that the total area of the 10 largest clusters is one measure for quantifying the extent of clustering. We normalize this area by the total area occupied by all the cells/clusters in the image. The same procedure is repeated for 3 images from the same sample. The average and standard deviation are thus computed for the normalized areal fraction (%) of the 10 largest clusters. For the images in Figure 3.1, we calculate this area to be $5 \pm 3\%$ for blood + chitosan (Figure 3.1a) whereas it is substantially higher at $62 \pm 2\%$ for blood + hmC (Figure 3.1b).
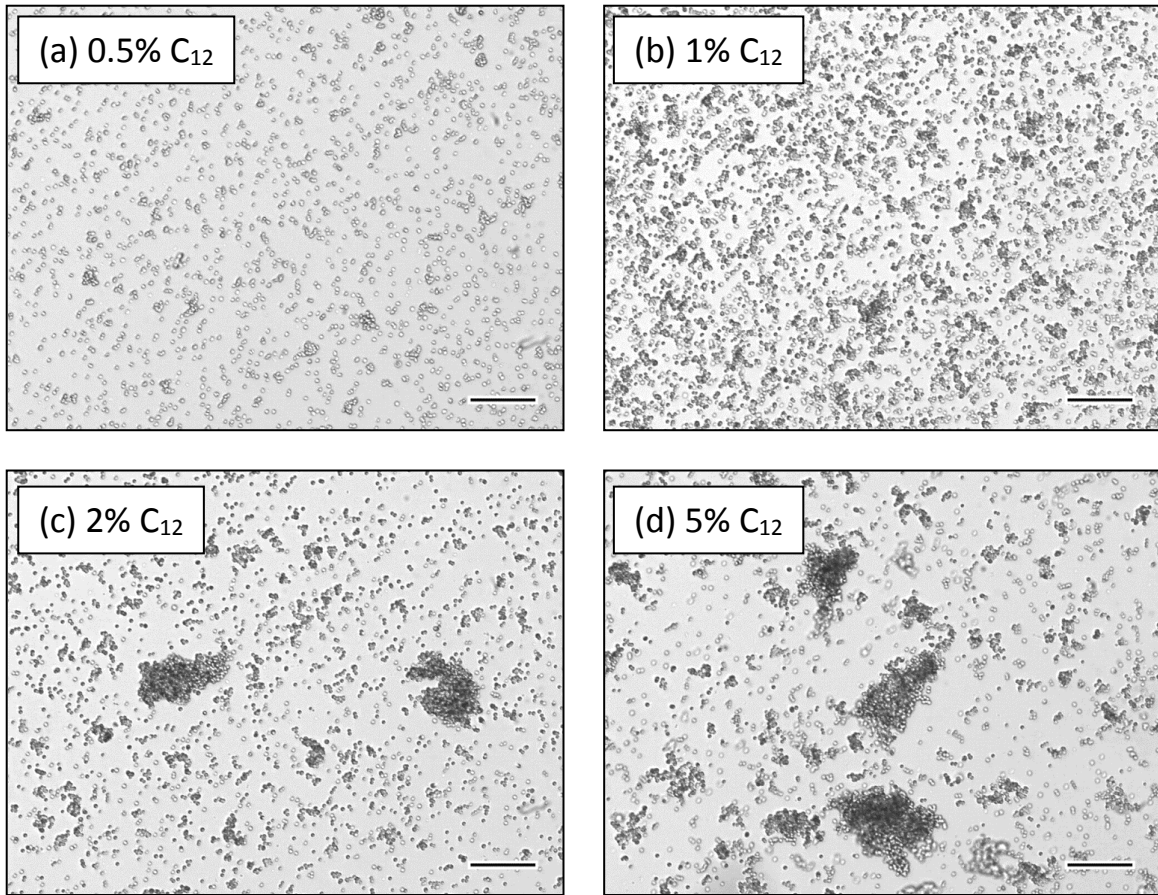
Figure 3.5 Effect of varying the degree of modification by C_{12} hydrophobes. Images are for citrated bovine blood combined with 0.05 wt% of hmC containing different mol% of C_{12} hydrophobes: (a) 0.5%; (b) 1%; (c) 2%; (d) 5%. Scale bars are 100 μm.
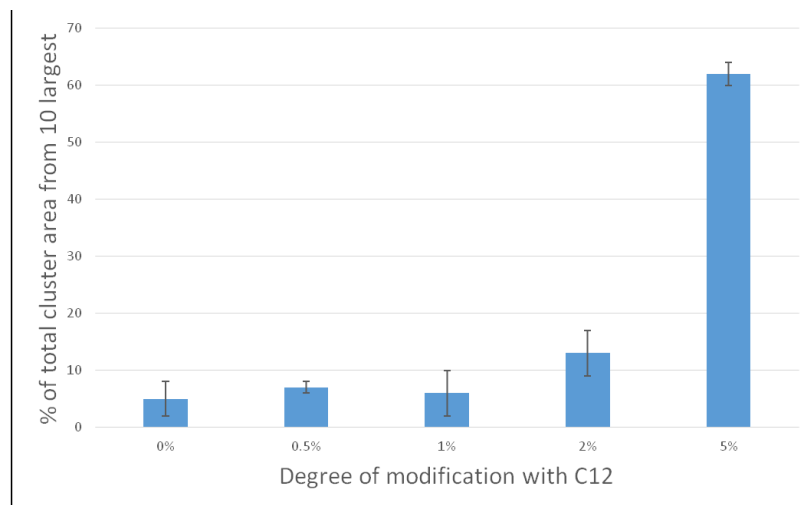
Figure 3.6 From the images in Figure 3.5, the areal fraction (%) of the 10 largest clusters is plotted against the degree of modification by C_{12} hydrophobes.

We now describe the effects of different variables on blood-cell clustering. First is the degree of hydrophobe modification, with the hydrophobe length maintained at C_{12}. We compared hmC variants with different degrees of C_{12} hydrophobes (0.5, 1, 2, and 5 mol% relative to the amine groups) with blood at a polymer concentration of 0.05 wt%. Figure 3.5 shows a systematic trend in the images, with the extent of blood-cell clustering increasing with the mol% of hydrophobes, i.e., the more the hydrophobes, the more the clustering. These images were quantified by the procedure described above, and the results for the areal fraction of the 10 largest clusters are presented in Figure 3.6. This parameter increases monotonically with increasing mol% of hydrophobes.
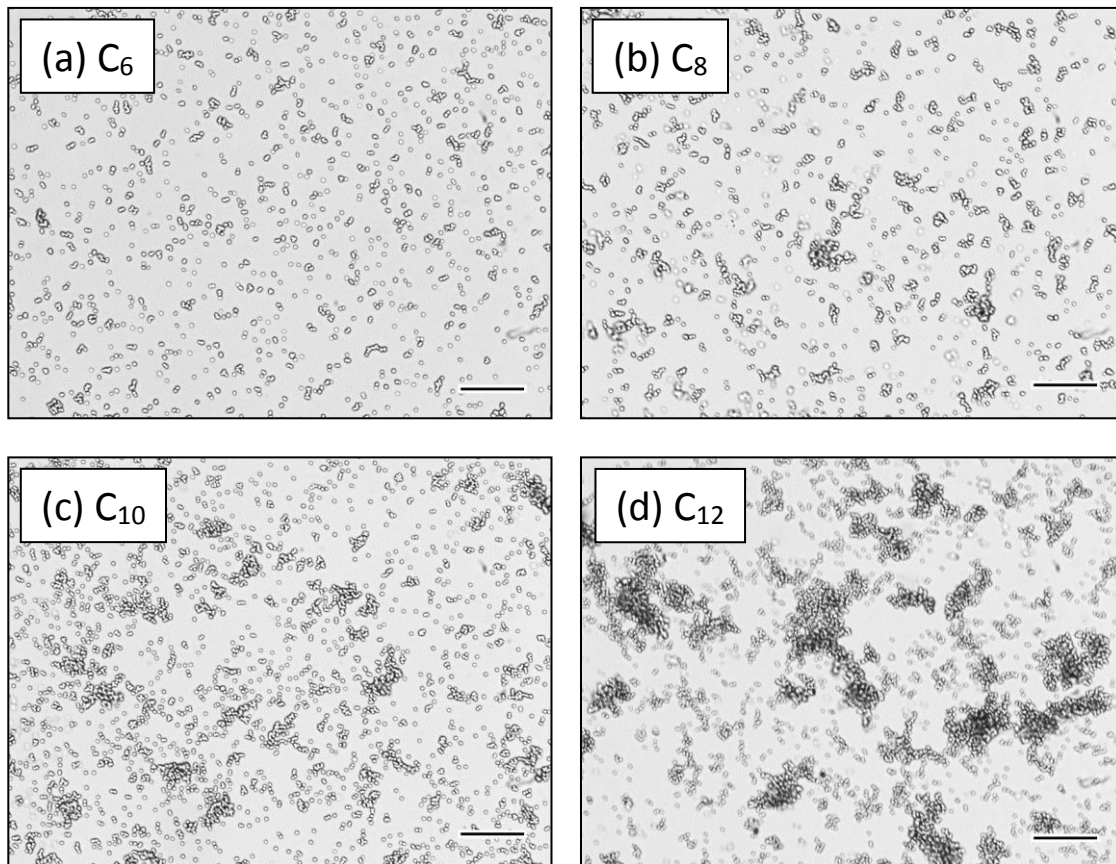
Figure 3.7 Effect of varying the length of hydrophobes. Images are for citrated bovine blood combined with 0.05 wt% of hmC containing different lengths of hydrophobes (5 mol% modification): (a) C_6; (b) C_8; (c) C_{10}; (d) C_{12}. Scale bars are 100 μm.

Figure 3.8 From the images in Figure 3.7, the areal fraction (%) of the 10 largest clusters is plotted against the hydrophobe length.

Next, we tested *n*-alkyl hydrophobes of different lengths (C_6, C_8, C_{10}, C_{12}). Different varieties of hmC with each of these hydrophobes were synthesized, with the degree of modification kept constant at 5 mol% relative to the amine groups. The different polymers were tested with blood at a polymer concentration of 0.05 wt%. Figure 3.7 again shows a systematic trend in the images, with clustering increasing with the length of hydrophobes. From these images, the areal fractions of the 10 largest clusters were extracted, and as expected, it increases monotonically with hydrophobe length (Figure 3.8).
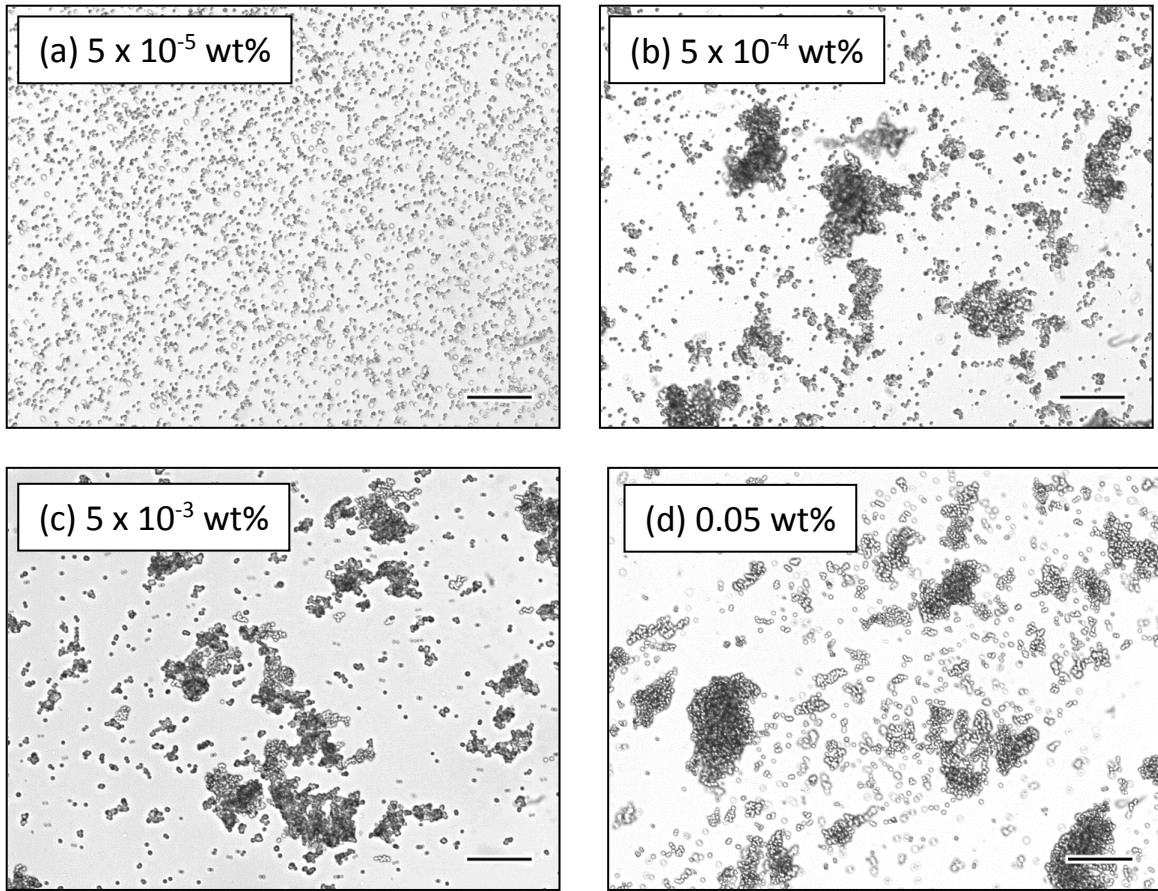
Figure 3.9 Effect of hmC concentration. Images are for citrated bovine blood combined with hmC (C_{12}, 5 mol%) at different concentrations: (a) 5×10^{-5} wt%; (b) 5×10^{-4} wt%; (c) 5×10^{-3} wt%; (d) 5×10^{-2} wt%. Scale bars are 100 μm.
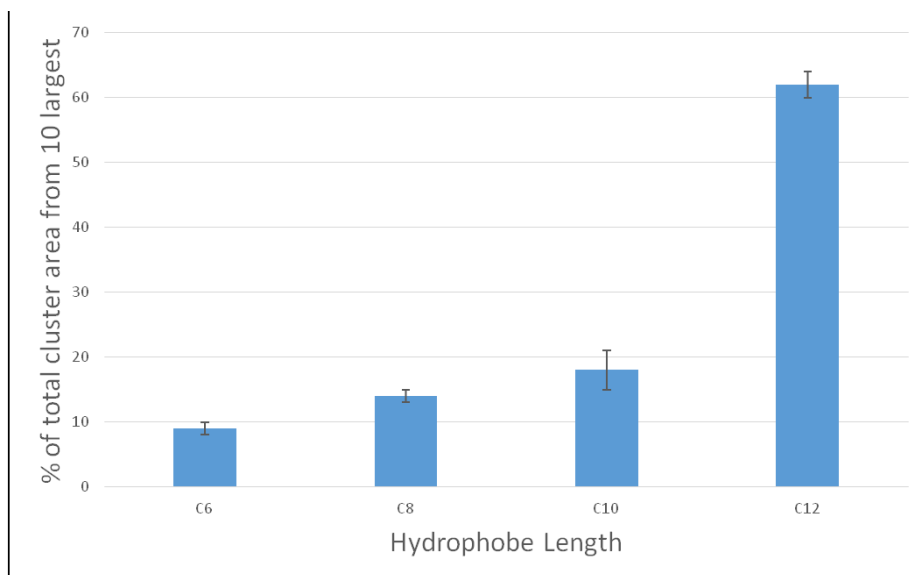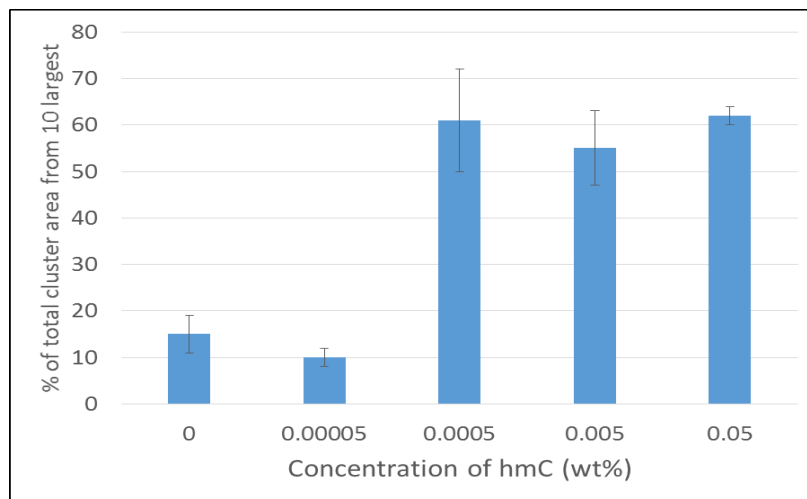

Figure 3.10 From the images in Figure 3.9, the areal fraction (%) of the 10 largest clusters is plotted against the hmC concentration.

Next, we examined different concentrations of an hmC with 5 mol% of C_{12} hydrophobes. The images in Figure 3.9 show that clustering occurs at hmC concentrations as low as 5×10^{-4} wt%. Moreover, the extent of clustering, in terms of the areal fractions of the 10 largest clusters, was indistinguishable for concentrations between 5×10^{-4} and 0.05 wt% (i.e., over two orders of magnitude). Thus, for a strongly clustering polymer like the hmC tested here (with a large number of long hydrophoobes), there appears to be a threshold concentration beyond which clustering is significant.
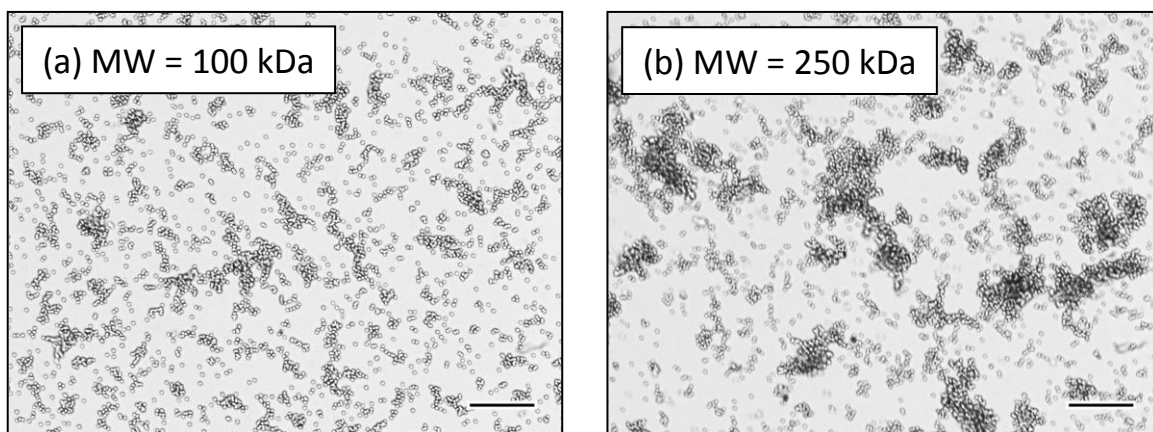
Figure 3.11 Effect of hmC molecular weight. Images are for citrated bovine blood combined with 0.05 wt% of hmC (C_{12}, 5 mol%) at two different molecular weights: (a) 100 kDa; and (b) 250 kDa. Scale bars are 100 μm.

The molecular weight (MW) of the hmC was also tested as an additional parameter. The polymers studied thus far had a molecular weight of 250 kDa. For comparison, we obtained a lower MW of chitosan, i.e., 100 kDa, and converted this to an hmC with 5 mol% of C_{12} hydrophobes. The two polymers were combined with blood at a concentration of 0.05 wt%. Figure 3.11 shows that the clustering in the case of the 100 kDa polymer is lower than in the case of the 250 kDa polymer. The areal fraction of

the 10 largest clusters was $22 \pm 3\%$ for the 100 kDa hmC compared to $62 \pm 2\%$ for the

250 kDa hmC.
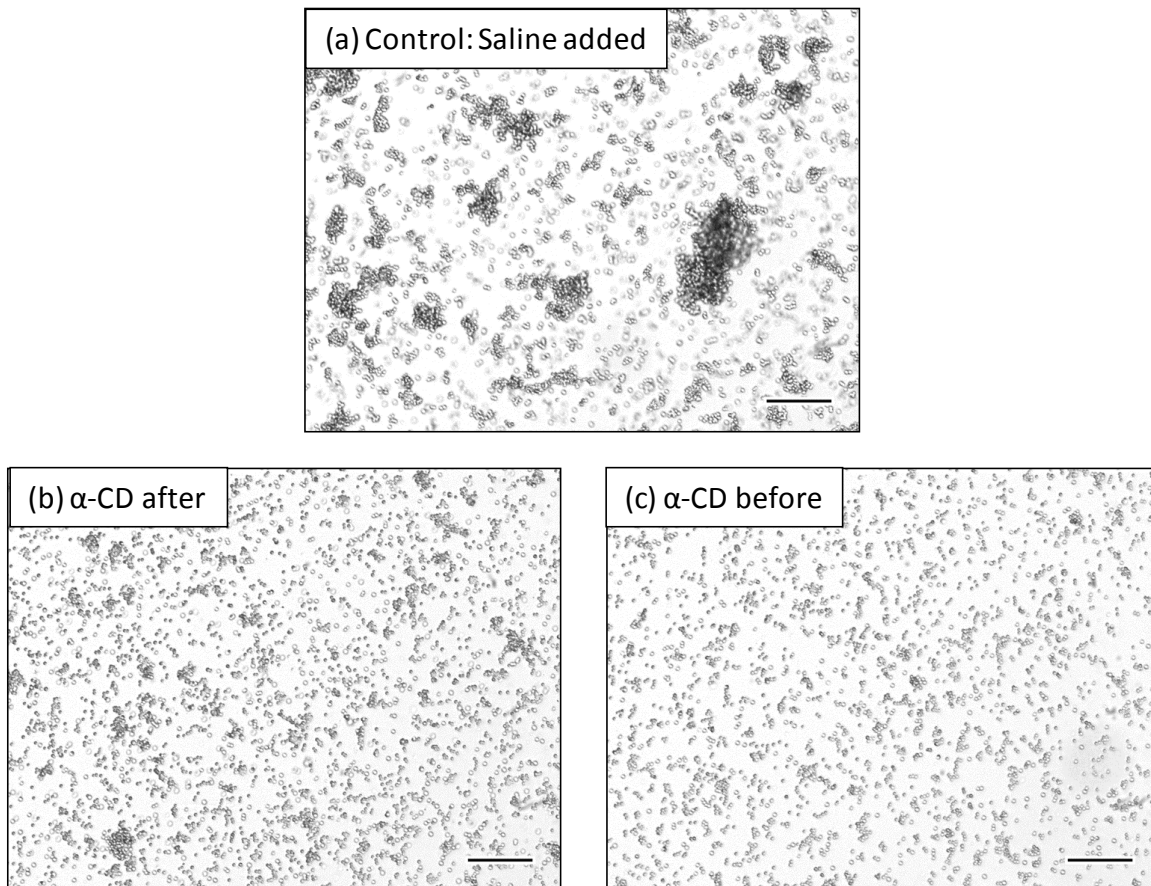
Figure 3.12 Effect of α-CD on the clustering of citrated bovine blood cells due to hmC (C_{12}, 5 mol%). (a) Control case: blood combined with hmC, then saline is added. (b) Blood combined with hmC, afterwards α-CD is added. (c) hmC is first combined with α-CD, then the mixture is combined with blood. In all three samples, the hmC concentration is the same (0.033 wt%), while in (b) and (c), the α-CD concentration is the same (16.7 mM). Scale bars are 100 μm.

We now examine whether clustering can be reversed by adding CDs. Specifically,

the type of CD that was shown to reverse gelation of blood (or vesicles) in past studies

was α-CD. Our first experiment involved mixing 20 μL each of blood and hmC solution

on the microscope slide (causing cells to cluster), and thereafter adding 20 µL of α-CD

solution. As a control, we substituted the α-CD solution with saline, and the result for

this case (blood + 0.033 wt% hmC) is shown in Figure 3.12a. As expected, we see

significant clustering. Next, Figure 3.12b shows an image of the sample with added

16.7 mM of α-CD. In this case, we see that the α-CD substantially reduces (but does not

eliminate) the clustering. Interestingly, the order of addition makes a difference. We

repeated the above experiment by first pre-mixing the hmC solution with the α-CD and

then adding this combination to blood (final sample has same concentrations of hmC and

α-CD). In this case, the clustering is almost eliminated, as shown in Figure 3.12c.
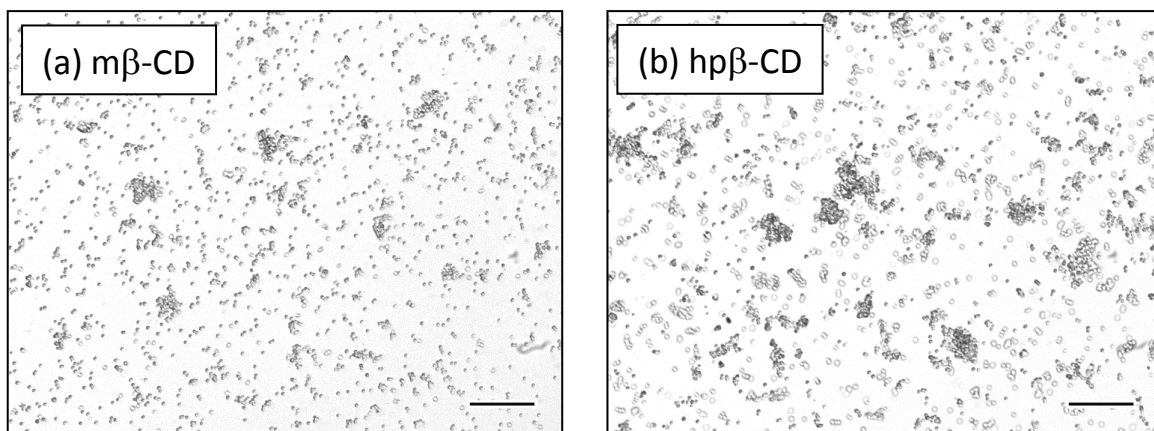
Figure 3.13 Effects of mβ-CD (a) and hpβ-CD (b) on the clustering of citrated bovine blood cells due to hmC (C_{12}, 5 mol%). In these experiments, hmC was first combined with the CD, and then the mixture was combined with blood. The hmC concentration in the two samples is 0.033 wt% while the CD concentration in each case is 16.7 mM. Scale bars are 100 µm.

We also compared other types of CDs for their ability to eliminate blood cell

clustering. Results for two derivatives of β-CD, i.e., mβ-CD and hpβ-CD, are shown in

Figure 3.13. In these experiments, the CD was premixed with the hmC and then added to

blood (same conditions as in Figure 3.12c). We note that both CDs reduce the clustering compared to that in the control (Figure 3.12a), but many clusters still do exist. Thus, neither of these CDs is as effective as α-CD in terms of eliminating clustering.

The experiments thus far have shown that hmC induces clustering of blood cells, with the clustering increasing with polymer MW and concentration, as well as with hydrophobe density and length. In addition, CDs, and in particular α-CD, reduce or eliminate the clustering. We can thus make a direct correlation between the clustering observed in our microscopic experiments and the gelation seen in macroscopic rheological experiments. Similarly the reversal of clustering by the CDs in the microscopic images corresponds to the reversal of gelation in the macroscopic studies.

Note that the microscopic experiments here have been done with diluted samples relative to those for which gelation is seen. Specifically, the blood cell density is diluted 10× relative to the original. Also, typical hmC concentrations for gelation with blood are about 0.25 to 0.5 wt% (in the case of an hmC with 5 mol% of C_{12} hydrophobes), which is 2 to 5× the concentrations studied here. As mentioned, direct microscopic studies are difficult for non-diluted samples because the high cell density obscures the field of view. Nevertheless, it is reasonable to conclude that clustering in a dilute mixture of hmC and blood goes hand-in-hand with gelation in more concentrated mixtures. In our images, the clusters are discrete; while such clustering will increase the sample viscosity, it will not lead to elastic rheology. Conversely, gelation will occur when a network of clusters is

formed that spans the entire sample volume. Such a network will respond as a single unit and in an elastic fashion at low deformations, thereby giving rise to a gel-like response.
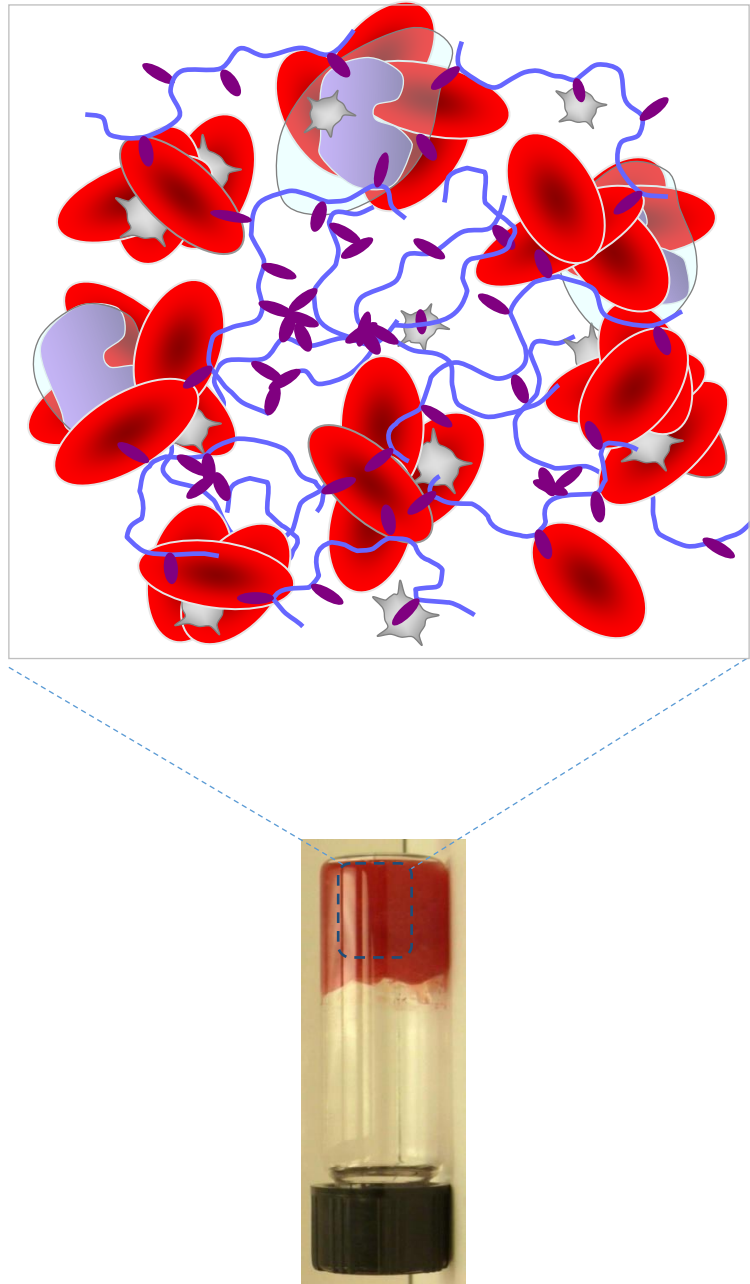
Figure 3.14 Proposed revised mechanism of gelation of hm-chitosan and blood mixtures. Hydrophobes insert into the membranes of red cells, white cells, and platelets, forming clusters which crosslink the polymer chains thus forming a gel. Hydrophobes also interact with other hydrophobes, further crosslinking the network.

Based on our results, we can propose a modified schematic representation for the microstructure of a blood/hmC gel. This is shown in Figure 3.14 and is to be compared with the schematic proposed earlier and shown in Figure 2.2b. In the new schematic, we envision the network as arising from cluster-cluster aggregation. In the colloid literature, there are models for diffusion-limited cluster-cluster aggregation, which lead to network structures that are rather similar to the above.[39,40] The key point here is that hmC seems to induce rather dense clusters of blood cells, as shown by our microscopic images. Such clusters are evidently formed by hydrophobic interactions, which is why the extent of clustering increases with hydrophobe length and density. We speculate that such clusters will serve as the nodes of a polymer/cell network. In our earlier mechanism, we had omitted such clusters and envisioned individual cells as the network nodes,[10] but this does not seem realistic based on our new data.

One other element that is reflected in our new schematic is the presence of hydrophobic associations between adjacent hmC chains. Such hydrophobic associations are usually thought to be transient structures. However, if their lifetimes are sufficiently high, they could contribute as additional crosslinks in the network. The reason for invoking these polymer-polymer interactions is two-fold. First, we observe that the addition of salt can significantly increase the viscosity of an hmC solution. This increase is evidently due to polymer-polymer hydrophobic interactions. Note that in the absence of salt, the polymer chains would experience significant electrostatic repulsions; however, salt ions screen these repulsions and allow the hydrophobes to interact with one another. Since salt is always present in blood plasma, its effect cannot be ignored. The

second issue has to do with the geometry of the system. For gelation to occur, the volume fraction of the cells must be such that the cells fill up the entire volume. However, if dense clusters are formed, the volume fraction is reduced and can be far from close-packing. In such a scenario, the polymer-polymer interactions can still contribute to the creation of a volume-filling network, as indicated in macroscopic experiments.

3.4 Conclusions

This work clearly demonstrates that hmC causes significant clustering and aggregation of the blood cells, which is not the case with chitosan. We have also demonstrated that the level of hydrophobic modification has a strong effect on the level of clustering observed. Higher levels of hydrophobic modification lead to higher levels of clustering. We have also shown the length of the hydrophobic group grafted onto the chitosan back bone plays a significant role in clustering. Chitosan modified with longer, more hydrophobic groups produced stronger clustering than short hydrophobes.

With respect to α-CD, we have shown that the introduction of α-CD can disrupt clustering almost completely. We also demonstrated that other cyclodextrins have a similar effect. Finally, we demonstrated a slight difference based on the order of addition of α-CD, in which α-CD introduced after clusters had already formed resulted in a small amount of clustering remaining in the sample.

Chapter 4: CONCLUSIONS & RECOMMENDATIONS

4.1 Conclusions

The motivation for this work was to further elucidate the mechanism of gelation between hmC and blood. In this work, we have utilized optical microscopy to observe and examine a dramatic difference in the clustering of blood cells when they are exposed to hmC compared to unmodified chitosan. To account for this clustering effect, we suggest a revision to the mechanism for the interaction of blood cells and hmC. This mechanism is one in which blood cells are found in clustered groups as opposed to singly, and where hydrophobe-hydrophobe interactions dominate in the space between adjacent clusters. In light of these conclusions, we describe a number of additional experiments to further elucidate the mechanism of gelation of hmC with blood and further explain the clustering observed in this thesis, as described below.

4.2 Future Directions

Chitosanase. One interesting avenue to pursue in continuing this line of research would be to investigate the effect of the enzyme chitosanase on the clustering observed between hm-chitosan and blood. Chitosanase is an enzyme that breaks down the chitosan polymer backbone. It is possible that by adding chitosanase into a sample containing clustered blood cells (due to the presence of hmC), the chitosanase will break down the hmC polymer and thereby decluster the blood cells. If this is the case, it would also be interesting to determine the minimum amount of chitosanase required for declustering.

Fluorescence. Another possible avenue to pursue would be to fluorescently label hmC with fluorescein groups. It is also possible to stain the membranes of red blood cells using lipid soluble dye such as Nile Red. This makes possible a wide range of experiments for further investigating the interaction between blood and hmC. For example, if both the blood cells and chitosan were labeled, confocal microscopy could be used to create a 3-D image of the hmC blood cell clusters. From these images, it could be determined where the hmC is relative to the blood cells.

Calcium Chloride. Sodium citrate was used in this study as an anticoagulant to prevent the blood from clotting due to the natural clotting cascade. Citrate works as an anticoagulant by chelating the calcium in blood. Since calcium is essential to natural clotting, chelating the calcium prevents clot formation. However, if additional calcium is added in to citrated blood, the chelation due to citrate is overloaded, and the extra calcium allows the natural clotting cascade to begin.

It would be interesting to use microscopy to observe blood cells that are clotted naturally. This could be done with whole blood, and also with diluted blood similar to what was used in this study. It is not certain that diluted blood would clot naturally, as all clotting factors would be diluted. However, it may be possible to resolve this by diluting blood using blood plasma as the diluent, which would preserve the concentrations of naturally clotting factors while still reducing the number of blood cells present in a sample.

With micrographs of naturally clotted blood, we could compare the images to those in this study with clustered blood cells due to the presence of hmC. It would be interesting to see if clusters are present in naturally clotted blood. If there are indeed clusters present, it would be interesting to do image analysis on those clusters and see how they compare to the clusters formed by hmC.

Time-Based Observations. As it has been previously indicated that chitosan can cluster blood cells over time, we recommend time based observations of all samples tested in this thesis. Samples of chitosan and hmC should be mixed with blood and observed at different time points up to at least two hours, as this was the time reported by Evans and Kent that it took for chitosan to cause blood cell clustering.[41]

REFERENCES

[1]   English, R. J.; Raghavan, S. R.; Jenkins, R. D.; Khan, S. A. "Associative polymers bearing n-alkyl hydrophobes: Rheological evidence for microgel-like behavior." *Journal of Rheology* **1999**, *43*, 1175-1194.

[2]   Panmai, S.; Prud'homme, R. K.; Peiffer, D. G. "Rheology of hydrophobically modified polymers with spherical and rod-like surfactant micelles." *Colloids and Surfaces a-Physicochemical and Engineering Aspects* **1999**, *147*, 3-15.

[3]   Desbrieres, J.; Martinez, C.; Rinaudo, M. "Hydrophobic derivatives of chitosan: Characterization and rheological behaviour." *International Journal of Biological Macromolecules* **1996**, *19*, 21-28.

[4]   Ashbaugh, H. S.; Boon, K.; Prud'homme, R. K. "Gelation of catanionic vesicles by hydrophobically modified polyelectrolytes." *Colloid and Polymer Science* **2002**, *280*, 783-788.

[5]   Bratskaya, S.; Avramenko, V.; Schwarz, S.; Philippova, I. "Enhanced flocculation of oil-in-water emulsions by hydrophobically modified chitosan derivatives." *Colloids and Surfaces a-Physicochemical and Engineering Aspects* **2006**, *275*, 168-176.

[6]   Chen, Y. J.; Javvaji, V.; MacIntire, I. C.; Raghavan, S. R. "Gelation of Vesicles and Nanoparticles Using Water-Soluble Hydrophobically Modified Chitosan." *Langmuir* **2013**, *29*, 15302-15308.

[7]   Chiu, Y.-L.; Chen, M.-C.; Chen, C.-Y.; Lee, P.-W.; Mi, F.-L.; Jeng, U. S.; Chen, H.-L.; Sung, H.-W. "Rapidly *in situ* forming hydrophobically-modified chitosan hydrogels via pH-responsive nanostructure transformation." *Soft Matter* **2009**, *5*, 962-965.

[8]   Cooney, M. J.; Petermann, J.; Lau, C.; Minteer, S. D. "Characterization and evaluation of hydrophobically modified chitosan scaffolds: Towards design of enzyme immobilized flow-through electrodes." *Carbohydrate Polymers* **2009**, *75*, 428-435.

[9]   Dowling, M. B.; Javvaji, V.; Payne, G. F.; Raghavan, S. R. "Vesicle capture on patterned surfaces coated with amphiphilic biopolymers." *Soft Matter* **2011**, *7*, 1219-1226.

[10]   Dowling, M. B.; Kumar, R.; Keibler, M. A.; Hess, J. R.; Bochicchio, G. V.; Raghavan, S. R. "A self-assembling hydrophobically modified chitosan capable of reversible hemostatic action." *Biomaterials* **2011**, *32*, 3351-3357.

[11]   Iversen, C.; Kjoniksen, A. L.; Nystrom, B.; Nakken, T.; Palmgren, O.; Tande, T. "Linear and nonlinear rheological responses in aqueous systems of hydrophobically modified chitosan and its unmodified analogue." *Polymer Bulletin* **1997**, *39*, 747-754.

[12]   Lee, J. H.; Agarwal, V.; Bose, A.; Payne, G. F.; Raghavan, S. R. "Transition from unilamellar to bilamellar vesicles induced by an amphiphilic biopolymer." *Physical Review Letters* **2006**, *96*.

[13]   Lee, J. H.; Gustin, J. P.; Chen, T. H.; Payne, G. F.; Raghavan, S. R. "Vesicle-biopolymer gels: Networks of surfactant vesicles connected by associating biopolymers." *Langmuir* **2005**, *21*, 26-33.

[14]   Tharanathan, R. N.; Kittur, F. S. "Chitin--the undisputed biomolecule of great potential." *Crit Rev Food Sci Nutr* **2003**, *43*, 61-87.

[15]   Javvaji, V.; Dowling, M. B.; Oh, H.; White, I. M.; Raghavan, S. R. "Reversible gelation of cells using self-assembling hydrophobically-modified biopolymers: towards self-assembly of tissue." *Biomaterials Science* **2014**, *2*, 1016-1023.

[16]   Antunes, F. E.; Coppola, L.; Rossi, C. O.; Ranieri, G. A. "Gelation of charged bio-nanocompartments induced by associative and non-associative polysaccharides." *Colloids and Surfaces B-Biointerfaces* **2008**, *66*, 134-140.

[17]   Chieng, Y. Y.; Chen, S. B. "Rheological study of hydrophobically modified hydroxyethyl cellulose and phospholipid vesicles." *Journal of Colloid and Interface Science* **2010**, *349*, 236-245.

[18]   Himmelein, S.; Lewe, V.; Stuart, M. C. A.; Ravoo, B. J. "A carbohydrate-based hydrogel containing vesicles as responsive non-covalent cross-linkers." *Chemical Science* **2014**, *5*, 1054-1058.

[19]   Liao, D.; Dai, S.; Tam, K. C. "Influence of anionic surfactant on the rheological properties of hydrophobically modified polyethylene-oxide/cyclodextrin inclusion complexes." *Journal of Rheology* **2009**, *53*, 293-308.

[20]   "Global, regional, and national age-sex specific all-cause and cause-specific mortality for 240 causes of death, 1990-2013: a systematic analysis for the Global Burden of Disease Study 2013." *Lancet* **2015**, *385*, 117-71.

[21]   Rhee, P.; Joseph, B.; Pandit, V.; Aziz, H.; Vercruysse, G.; Kulvatunyou, N.; Friese, R. S. "Increasing trauma deaths in the United States." *Ann Surg* **2014**, *260*, 13-21.

[22]   Champion, H. R.; Bellamy, R. F.; Roberts, C. P.; Leppaniemi, A. "A profile of combat injury." *J Trauma* **2003**, *54*, S13-9.

[23]   Kauvar, D. S.; Lefering, R.; Wade, C. E. "Impact of hemorrhage on trauma outcome: an overview of epidemiology, clinical presentations, and therapeutic considerations." *J Trauma* **2006**, *60*, S3-11.

[24]   Kelly, J. F.; Ritenour, A. E.; McLaughlin, D. F.; Bagg, K. A.; Apodaca, A. N.; Mallak, C. T.; Pearse, L.; Lawnick, M. M.; Champion, H. R.; Wade, C. E.; Holcomb, J. B. "Injury severity and causes of death from Operation Iraqi Freedom and Operation Enduring Freedom: 2003-2004 versus 2006." *J Trauma* **2008**, *64*, S21-6; discussion S26-7.

[25]   Martin, M.; Oh, J.; Currier, H.; Tai, N.; Beekley, A.; Eckert, M.; Holcomb, J. "An analysis of in-hospital deaths at a modern combat support hospital." *J Trauma* **2009**, *66*, S51-60; discussion S60-1.

[26]   Stewart, R. M.; Myers, J. G.; Dent, D. L.; Ermis, P.; Gray, G. A.; Villarreal, R.; Blow, O.; Woods, B.; McFarland, M.; Garavaglia, J.; Root, H. D.; Pruitt, B. A., Jr. "Seven hundred fifty-three consecutive deaths in a level I trauma center: the argument for injury prevention." *J Trauma* **2003**, *54*, 66-70; discussion 70-1.

[27]   De Castro, G. P.; Dowling, M. B.; Kilbourne, M.; Keledjian, K.; Driscoll, I. R.; Raghavan, S. R.; Hess, J. R.; Scalea, T. M.; Bochicchio, G. V. "Determination of efficacy of novel modified chitosan sponge dressing in a lethal arterial injury model in swine." *J Trauma Acute Care Surg* **2012**, *72*, 899-907.

[28]   Dowling, M. B.; MacIntire, I. C.; White, J. C.; Narayan, M.; Duggan, M. J.; King, D. R.; Raghavan, S. R. "Sprayable Foams Based on an Amphiphilic Biopolymer for Control of Hemorrhage Without Compression." *Biomaterials* **In prep**.

[29]   Dowling, M. B.; Smith, W.; Balogh, P.; Duggan, M. J.; MacIntire, I. C.; Harris, E.; Mesar, T.; Raghavan, S. R.; King, D. R. "Hydrophobically-modified chitosan foam: description and hemostatic efficacy." *J Surg Res* **2015**, *193*, 316-23.

[30]   Elsabee, M. Z.; Abdou, E. S. "Chitosan based edible films and coatings: a review." *Mater Sci Eng C Mater Biol Appl* **2013**, *33*, 1819-41.

[31]   Raafat, D.; von Bargen, K.; Haas, A.; Sahl, H. G. "Insights into the mode of action of chitosan as an antibacterial compound." *Appl Environ Microbiol* **2008**, *74*, 3764-73.

[32]   Rabea, E. I.; Badawy, M. E.; Stevens, C. V.; Smagghe, G.; Steurbaut, W. "Chitosan as antimicrobial agent: applications and mode of action." *Biomacromolecules* **2003**, *4*, 1457-65.

[33] Raftery, R.; O'Brien, F. J.; Cryan, S. A. "Chitosan for gene delivery and orthopedic tissue engineering applications." *Molecules* **2013**, *18*, 5611-47.

[34] Goy, R. C.; Britto, D. d.; Assis, O. B. G. "A review of the antimicrobial activity of chitosan." *Polímeros* **2009**, *19*, 241-247.

[35] Kheirabadi, B. S.; Scherer, M. R.; Estep, J. S.; Dubick, M. A.; Holcomb, J. B. "Determination of efficacy of new hemostatic dressings in a model of extremity arterial hemorrhage in swine." *J Trauma* **2009**, *67*, 450-9; discussion 459-60.

[36] Wollman, A. J.; Nudd, R.; Hedlund, E. G.; Leake, M. C. "From Animaculum to single molecules: 300 years of the light microscope." *Open Biol* **2015**, *5*.

[37] Pons, M. N.; Vivier, H. "Biomass quantification by image analysis." *Adv Biochem Eng Biotechnol* **2000**, *66*, 133-84.

[38] Turgeon, M. L. *Clinical Hematology: Theory and Procedures*; Lippincott Williams & Wilkins, 2005.

[39] Meakin, P. "Effects of cluster trajectories on cluster-cluster aggregation: A comparison of linear and Brownian trajectories in two- and three-dimensional simulations." *Physical Review A* **1984**, *29*, 997-999.

[40] Meakin, P.; Vicsek, T.; Family, F. "Dynamic cluster-size distribution in cluster-cluster aggregation: Effects of cluster diffusivity." *Physical Review B* **1985**, *31*, 564-569.

[41] Evans, E. E.; Kent, S. P. "Use of basic polysaccharides in histochemistry and cytochemistry, precipitation and agglutination of biological materials by aspergillus polysaccharide and deacetylated chitin." *Journal of Histochemistry & Cytochemistry* **1962**, *10*, 24-&.